RESISTANCE OF CHLORIDE AND SULFATE OF GEOPOLYMER MORTAR BASED ON FLY ASH AND SILICA FUME AS ALTERNATIVE RAW MATERIALS

Sirirat Tubsungnoen Rattanachan*, Rawee Dangwiriyakul, Oranich Thongsri, Paritat Thaitalay and Sawitri Srisuwan

Received: April 25, 2023; Revised: July 07, 2023; Accepted: August 15, 2023

Abstract

The durability of concrete in acid or salt environments greatly influences its service life. This paper aims to develop the mortar composition for chloride and sulfate salt resistance at 50,000 mg/L as the simulated salt solution. Geopolymer mortar in this study consisted of 10%weight ordinary Portland cement (OPC type 1) with the other alternative raw materials which were pozzolanic materials and wastes (fly ash, silica fume and rice husk ash). Several parameters were investigated, including the type and content of the alternative raw materials, liquid to powder ratio, to enhance the compressive strength of the geopolymer mortar after a 14-day immersion in the simulated salt solution as comparison with those in the normal water and the ordinary Portland cement. The results demonstrated that geopolymer mortar composed of fly ash and silica fume, with the mixture of NaOH (10M): Na_2SiO_3 in ratio of 24:16 (wt/wt), exhibited the improvement of the compressive strength as compared to ordinary Portland cement type 1 and type 5 after the 14-day exposured in salt environment. Moreover, this geopolymer mortar provided low density, making it suitable for engineering structures in high-salt areas. Furthermore, this paper investigated the chemical reactions and phases that occur in the geopolymer mortar upon setting in high concentrations of chloride and sulfate solutions by XRD and FESEM-EDS techniques. XRD and FESEM-EDS results indicated that the change of chemical reaction and phases after setting of geopolymer mortar in high concentrations of chloride and sulfate solution provided the protection of Mg and Cl ions penetration inside the samples better than the Ordinary mortar. These findings provide insights into the salt resistance mechanism of geopolymer and lay the groundwork for developing concrete compositions with improved salt resistance in the future.

Keywords: **Chloride resistance; fly ash; geopolymer; silica fume; sulfate resistance**

School of Ceramic Engineering, Institute of Engineering, Suranaree University of Technology, 111 University, Avenue, Muang District, Nakhon Ratchasima 30000, Thailand. E-mail: sirirat.b@g.sut.ac.th; mos_rawee@hotmail.com; oranich.ts@gmail.com; prem_pukkylover@hotmail.com; sawitri.sr@gmail.com

* *Corresponding author*

DOI: https://doi.org/10.55766/sujst-2023-05-e01092

Suranaree J. Sci. Technol. 30(5):030147(1-9)

Introduction

Globally, depending on the geographic area and farming activities, many areas occupied a high concentration of salt solution (Nagaraju *et al.*, 2022). Those areas can harm the environment and buildings, degrade the mechanical properties, and decrease the life expectancy of structural engineering. Building materials with high salt resistance are interesting to develop and improve the quality of ordinary building materials. Global warming with issue of CO_2 emissions by cement production trend to the development of geopolymer. Geopolymer are three-dimensional amorphous to semi-crystalline aluminosilicate formed from raw materials rich in silica and aluminium (Davidovits, 1994; Krishnam Raju *et al.*, 2023; Nagaraju *et al.*, 2023a). Geopolymer technology also can reduce global greenhouse emissions caused by OPC production (Živica *et al.*, 2024). Due to the high mechanical properties of geopolymer cements and its environmentally beneficial technology they appear as a prospective construction material for the future (Singh and Middendorf, 2020; Sambucci *et al.*, 2021; Nagaraju *et al.*, 2023b). The replacement ratios from the cement content were 10, 20, and 30% respectively, for each recycle of rice husk ash (RHA) and fly ash (FA) from power plants as reactivity materials for producing sustainable concrete (Chaitanya *et al.*, 2023). The replacement ratios of 10 and 30% of RHA presented higher mechanical properties than those of FA for each group. The water permeability decreased as the cementitious content increased due to the decrease in air content for all mixtures. The water permeability loss ratios increased as the cementitious content decreased (Amin and Abdelsalam, 2019). The RHA and FA replacement ratios from cement contents were beneficial for decreasing the air content and water permeability of concrete mixtures. This result achieved the main goal by using high replacement ratios of RHA and FA for improving the durability of concrete.

Compressive strength increases with the increase in the percentage of FA and RHA up to replacement (22.5% FA and 7.5% RHA) of Cement in Concrete for different mix proportions. The water-cement ratio percentage relies on the quantity of RHA used in concrete. Because RHA is a highly porous material. The workability of concrete had been found to decrease with an increase in RHA in concrete (Sathawane *et al.*, 2013; Nagaraju *et al.*, 2023a). The study investigated the properties of blended geopolymer based on FA and RHA activated with sodium aluminate as an aluminium additive (Chanakya Varma *et al.*, 2023). Results showed that 25% replacement by RHA was the optimal percentage on physical-mechanical properties of the blended geopolymer (Chanakya Varma *et al.*, 2023). The finer particles of RHA filled the voids present in the geopolymer matrix through filling effect and enriched the gel, which densified the specimen. SEM micrographs also validated the denser matrix of the specimen at the optimal replacement percentage. However, it was seen that blending RHA with FA beyond the optimal 25% has a negative effect on the properties studied. The observation may be attributed due to the presence of zeolite X as confirmed by Quantitative XRD (Ken *et al.*, 2015). An increase in the amount of zeolite X and its crystalline size had a negative impact on the compressive strength of the blended geopolymer. The previous study was expected to provide a practical solution of utilizing FA and RHA solid waste in construction activities (Singh *et al.*, 2021). Results showed that the geopolymer concretes exhibited better corrosion resistance than OPC concrete. The higher the amount of Na_2SiO_3 and higher the concentration of NaOH solutions, the better the corrosion resistance of geopolymer concrete was (Shaikh, 2014). The test results confirmed that the mechanical properties of the geopolymer mixtures tested are competitive with those of OPC concrete and provide a more durable alternative to the OPC concrete in a seawater environment (Olivia and Nikraz, 2012).

In this study, it aims to develop the geopolymer mortar for chloride and sulfate resistance by replacement of the other alternative raw materials such as fly ash (FA), silica fume and rice husk ash (RHA) as well as rice husk ash calcined at the different temperatures. In this study, it was designed to use the ordinary Portland cement (OPC) in less amount and substitute it with waste or other alternative raw materials for cost-effectiveness and environment friendly. Only 10% weight of OPC in mortar composition was studied in this study. The chemical and phase analysis were provided for evaluating the reaction and the change of chemical composition during soaking in the high concentrations of chloride and sulfate solution as compared to ordinary Portland cement. It will bring the understanding of the corrosion mechanism and develop the new cement compositions.

Materials and Methods

Ordinary Portland cement under the brand name “Siam Cement Group”, was utilized as a cement or

Table 1. Composition of geopolymer samples

Sample code no.	Powder (%wt)								Liquid (g)		L/P ratio
	OPC1	OPC5	Fly ash	Silica fume	RHA	RHA500	RHA600	RHA700	Water	NaOH (10M):Na_2SiO_3 24 : 16 wt.) (g)	
T1	10 0								**40**	-	0.4
T5		100							40	-	0.4
FA	10		90							40	0.4
$FASiO_2$	10		85	5						40	0.4
FARHA	10		85		5					50	0.5
FARHA500	10		85			5				50	0.5
FARHA600	10		85				5			50	0.5
FARHA700	10		85					5		50	0.5

Table 2. Physical characteristics of raw materials

Raw materials	Density (g/cm^3)	Average particle size (μm)
Fly ash	1.94	40.32
Silica fume	2.23	35.81
RHA	1.97	106.09
RHA500	2.09	105.07
RHA600	2.15	101.16
RHA700	2.02	103.32

binding material. Portland cement type 1 was the general cement and Portland cement type 5 was the special sulphate resistance cement which was suitable for structural work near the sea or where the soil contains high salinity. Fly ash (FA) was collected from Mae Moh coal power plant, Lampang province in Thailand. The Mae Moh coal power plant generated about 20,000,000 Tons of fly ash annually, which are dumped in a landfill. The silica fume was purchased from Elkem. The rice husk was collected from the region of Nakhon Ratchasima. After its collection, the rice husk was burnt under uncontrolled burning temperatures to produce ash powder as received. The rice husk was heated at 500, 600, and 700°C in an electrical furnace at ambient atmosphere as denoted as RHA500, RHA600, and RHA700, respectively. Particle size distribution of all raw materials were characterized by using laser scattering particle size distribution analyzer (LA-950V2/Horiba) with a step time of 0.02º/min and a scan range of 10-70º. Chemical analysis of all raw materials was evaluated by X-ray fluorescence spectrometer (D2-phaser/ Bruker).

The true density of all raw materials was determined by gas pycnometer (multipycnometer/ Quantachrome). The oxide composition, density, and medium particle size of OPC, fly ash, silica fume, RHA and RHA heated at 500-700°C are presented in Table 2.

The cement composition composed of the Portland cement with the alternative raw materials for replacement of the Portland cement content such as fly ash, silica fume and rice husk ash for 10%wt. The liquid solution consisted of NaOH (10M): Na_2SiO_3 in ratio of 24:16 (wt/wt) solution. The liquid to powder ratio was 0.4-0.5 in the range. Geopolymer compositions were studied in this work as summarized in Table 1.

Geopolymer samples were prepared from the mixture of OCP and the alternative raw materials with the alkali solution. The cubic shape specimens with 50×50 mm in dimension were prepared for tests. Then, the samples were kept in mold for 1 day before demolded and wrapped by the plastic bag for curing in the hot oven at 60°C for 7 days. After 7 days of curing, the samples were soaked in different conditions (normal water and the simulated salt) for 14 days. The simulated salt was prepared from the solution of sodium chloride (NaCl) and magnesium sulphate ($MgSO_4$) for concentration of chloride and sulphate of 50,000 mg/L.

After soaking in the different conditions for 14 days, the samples were dried in air for 1 day. The density of all samples was determined as compared to those one before soaking in the different conditions. The compressive strength of specimens was tested by Universal testing machine (MUL-125 TTR/UTM capacity 100 kN) at cross speed of 1 mm/min-1. The value of compressive strength was the average of three specimens.

For further analysis, the outer and inner of all samples were characterized for chemical and microstructure analysis by using X-ray diffractometer (XRD) and Scanning electron microscopy with energy dispersive X-ray (SEM-EDS) techniques, respectively, to evaluate the effect of the alternative raw materials and geopolymer reactions on the different soaking conditions. The morphologies of geopolymer soaked in the different conditions were observed using Scanning electron microscopy with energy dispersive X-ray (SEM/EDX, JSM-6010LV/JEOL) at the accelerating voltage of 15 kV. An X-ray diffractometer (XRD, D2-phaser/Bruker) was used to analyze the components and crystalline phase variation of geopolymer with the Cu Kα radiation (λ = 1.5406 Å). The data were analysed in the range of 2θ from 10 to 70, and in increments of 0.02 with the counting time per step of 0.5. For XRD and SEM-EDX analyses, the upper portions of the specimens were sectioned into 5 mm thick plates using a diamond-crusted blade with a water-cooling system. The outer surface of the cut plate, which had direct contact with the solution, was designated as the "outside surface specimens". For the inside of specimens, a 5 mm thick plate was perpendicularly cut from the center of the specimen, referred to as "inside surface specimens" utilized for XRD and SEM-EDX analysis, as illustrated in Figure 1.

Results and Discussion

Chemical compositions of all raw materials in this study were characterized by X-ray fluorescence spectroscopy (XRF) as summarized in Table 3. OPC type 1 and type 5 presented high CaO and SiO_2 which were mainly acted as binder pozzolanic reaction. Fly ash provided high Al_2O_3 and SiO_2 contents. Silica fume and rice husk ash presented mainly high amorphous silica of 93.74% and 97.36%, respectively.

From the previous report (Jaya *et al.*, 2013), rice husk ash samples were prepared at different temperatures (600°C, 800°C, and 1,000°C) and it was partially replaced with OPC for 10%, 15%, 20%, and 30% by weight of OPC. It is clearly seen that the amorphous phases for RHA were produced at low temperatures of 600 and 800°C while the crystalline phase was observed at a higher temperature of 1,000°C. In this study, rice husk ash was burned at 500°C, 600°C, and 700°C because it required amorphous and removed almost residual

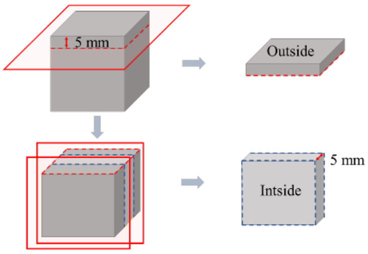

Figure 1. Specimen preparation for XRD and SEM-EDAX analyses

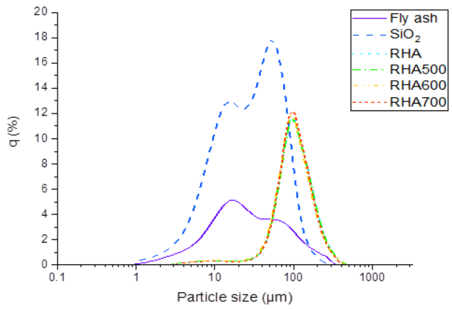

Figure 2. Particle size distribution of fly ash, silica fume, and RHA (as received) and RHA calcined at 500°C, 600°C, and 700°C

Table 3. Chemical analysis of raw materials for geopolymers

Elements (%)	Raw materials							
	OPC I	OPC V	Fly ash	Silica fume	RHA	RHA500	RHA600	RHA700
SiO_2	22.3	27.78	57.88	93.74	97.36	97.51	97.41	97.76
Al_2O_3	2.87	7.01	29.36	-	-	-	-	-
Fe_2O_3	4.03	7.41	5.52	4.04	0.18	0.08	0.08	0.08
CaO	60.36	45.47	3.19	0.88	0.37	0.37	0.34	0.34
Na_2O	2.81	4.03	-	-	-	-	-	-
K_2O	-	0.58	2.84	0.67	1.57	-	1.46	1.45
MgO	2.61	2.09	-	-	-	-	-	-
SO_3	3.03	4.87	-	-	-	-	-	-
TiO_2	0.25	0.31	-	-	-	-	-	-
Cr_2O_3	0.04	0.02	-	-	-	-	-	-
MnO_2	0.13	0.1	-	-	-	-	-	-
CuO	0.05	-	-	-	-	-	-	-
ZnO	0.45	0.08	-	-	-	-	-	-
SrO	0.27	-	-	-	-	-	-	-
Yb_2O_3	0.44	0.02	-	-	-	-	-	-
As_2O_5	-	0.01	-	-	-	-	-	-

carbon in the rice husk. The amorphous phase is very reactive and can considerably improve the strength of mortar and cement.

Density and average particle size of fly ash and all rice hush ash (as received, calcined at 500°C, 600°C, and 700°C) were presented in Table 2. All alternative raw materials have density in the range of 1.9-2.23 g/cm^3. Silica fume and fly ash showed the smallest average particle size of 35.81 μm and 40.32 μm, respectively. Moreover, average particle size of all rice husk ash was in range of 100-106 μm and their particle size distributions were presented in Figure 2. Rice husk ash showed the narrow particle size distribution while fly ash and silica fume showed the broad particle size distribution.

Effect of the Alternative Raw Materials Composition on the Density and Compressive Strength of the Geopolymer

Lightweight concrete with sulfate resistance cement has a few reports. The structural lightweight concrete with an ultra-high-performance matrix and expanded glass as a lightweight aggregate was studied and since the capillary porosity basically enables transport processes into the concrete, the material had to be examined more closely from the aspect of durability (Umbach *et al*., 2021). Another work (Bumanis *et al*., 2022) calcined illite or kaolin clay in combination with salt cake from the aluminium scrap recycling industry after alkali activation gives lightweight material from 540-675 kg/m^3. Sulfate attack showed significant strength loss for red clay based geopolymers after 61 days of soaking time in contrast to metakaolin-based geopolymers.

All geopolymer samples were determined the density before and after soaking in the different solutions as shown in Figure 3. It was evident that the density of geopolymer was lower compared to that of ordinary Portland cement, indicating its suitability for lightweight cement applications. Regarding the effects of water and salt solutions on the samples, Figure 3 indicates that the density of all samples increased after immersion in these solutions. However, there were no significant differences in density among the samples after immersion. This density increase can be attributed to phase formation during setting, wherein new

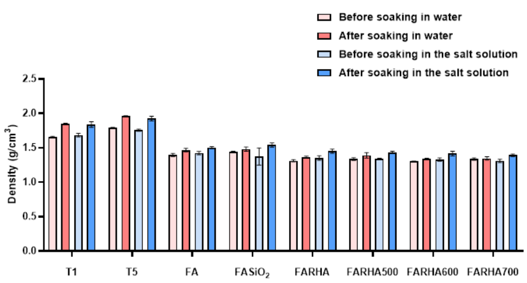

Figure 3. **Density of geopolymer samples before and after soaking in the different solutions (water and the simulated salt solution) for 14 days as compared to the ordinary Portland cement T1 and T5**

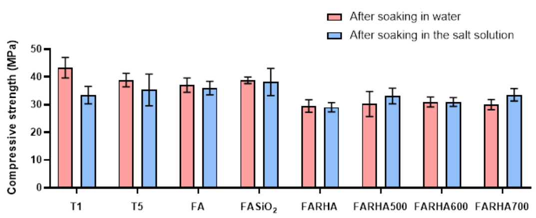

Figure 4. **Compressive strength of geopolymer samples before and after soaking in the different solutions (water and the simulated salt solution) for 14 days as compared to the ordinary Portland cement T1 and T5**

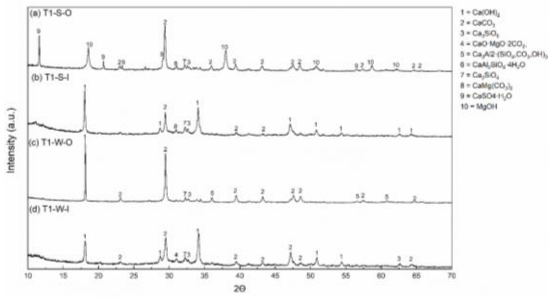

Figure 5. **XRD patterns of (a) surface, (b) inside of T1 sample soaked in the salt solution for 14 days and (c) surface and (d) inside of T1 sample soaked in water for 14 days**

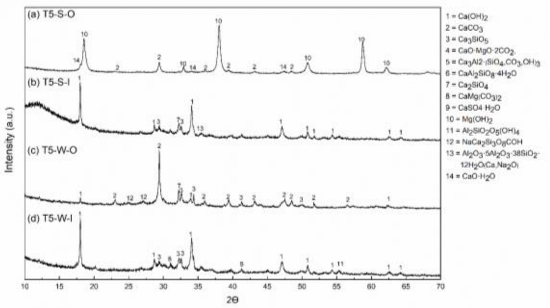

Figure 6. **XRD patterns of (a) surface, (b) inside of T5 sample soaked in the salt solution and (c) surface and (d) inside of T5 sample soaked in water for 14 days**

phases precipitated on the surface of the soaked samples. The different phases observed in the samples soaked in water and salt solution are illustrated in Figures 5-9.

After soaking in water and the salt solution for 14 days, the compressive strength of all geopolymer samples was determined as compared to the ordinary cement as shown in Figure 4. The result showed that the compressive strength of the ordinary cement T1 and T5 was decreased after soaking in the salt solution while the compressive strength of all geopolymer samples was not significantly decreased. It should be noted that the compressive strength of $FASiO_2$ geopolymer sample showed higher than that of the ordinary Portland cement for before and after soaking in the salt solution. This result can be indicated that geopolymer cements in this study were good salt resistance with high chloride and sulfate concentrations. Especially, FA and $FASiO_2$ geopolymers were interested in further examination for mechanism of salt resistance. For the mixing of FARHA, FARHA500, FARHA600 and FARHA700 pastes, it found that liquid to powder ratio must be increased to 0.5 which was higher than the others. RHA had high water absorption resulting in too hard for molding. This resulted in obtaining lower compressive strength for FARHA series. The compressive strength of FARHA, FARHA500, FARHA600 and FARHA700 samples showed lower than others.

Chemical Analysis of the Geopolymer with the Alternative Raw Materials Compositions on the Chloride and Sulfate Resistance

The chemical phase analysis of geopolymer samples was studied for understanding the hardening reactions as well as chloride and sulfate resistance as compared to the ordinary cement T1 and T5. The inside and outside of the sample soaked in the different solutions were characterized by SEM-EDS technique for microstructural examination and chemical analysis. Phases analysis of the ordinary cement T1 presented in XRD patterns as shown in Figure 5.

The main phases of T1 soaked in water for 14 days were $CaCO_3$ and $Ca(OH)_2$, especially inside of the samples showed much Ca $(OH)_2$ (Figure 5(d)). It found that the phase difference of T1 soaked in the salt solution which occurred $MgOH_2$ phase on the surface sample and much of $Ca(OH)_2$ as compared to those samples soaked in water. XRD patterns of inside of T5 specimens were not significantly difference between the soaking in water and in the salt solution as shown in Figures 6(b) and 6(d). However, it found a significant difference for samples outside of T5 soaked in

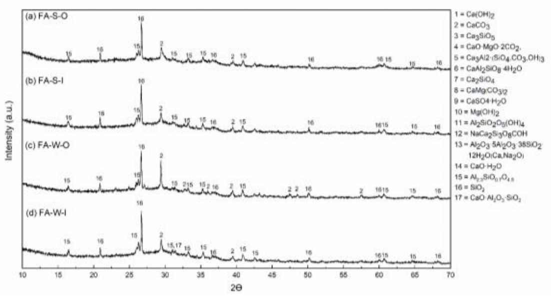

Figure 7. XRD patterns of (a) surface, (b) inside of FA geopolymer soaked in the salt solution and (c) surface and (d) inside of FA geopolymer soaked in water for 14 days

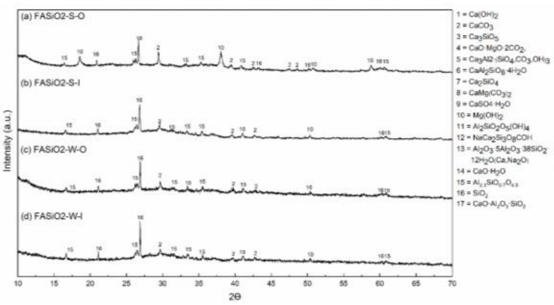

Figure 8. XRD patterns of (a) surface, (b) inside of $FASiO_2$ geopolymer soaked in the salt solution and (c) surface and (d) inside of $FASiO_2$ geopolymer soaked in water for 14 days

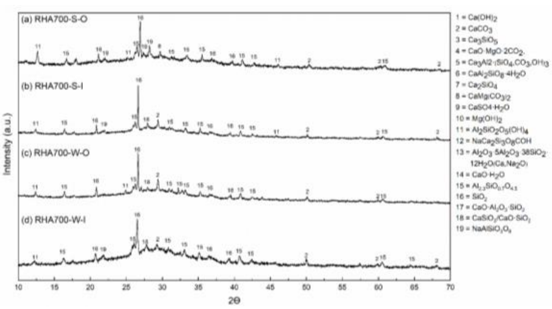

Figure 9. XRD patterns of (a) surface, (b) inside of RHA700 geopolymer soaked in the salt solution and (c) surface and (d) inside of RHA700 geopolymer soaked in water for 14 days

different conditions. The outside of T5 samples soaked in the salt solution observed $Mg(OH)_2$ as the main phase (Figure 6(a)). Phase analysis of FA geopolymer inside and outside samples soaked in the different solutions resulted in no significantly different among them as shown in Figure 7(a)-(d). While phase analysis of $FASiO_2$ geopolymers inside and outside samples soaked in the different solutions also showed not significantly difference (Figure 8) but it can be noticed that less $Mg(OH)_2$ was found on the outside $FASiO_2$ soaked in the salt solution for 14 days (Figure 8(a)). In addition, there was not a significantly different of phases analysis for RHA700 geopolymer inside and outside samples soaked in the different solutions as shown in Figure 9. However, RHA series showed poor compressive strength so that it was not interesting to study in the next experiment.

The geopolymerization process starts from alkaline activation of reactive alumino silicate materials as fly ash in an aqueous environment at pH >12, accompanied by hardening of cement. Then, calcium atoms present in the Si-O-Al-O skeleton structure and compensating the charge on aluminum atoms play a high strength of geopolymer cement (Meesala *et al*., 2020). RHA and silica fume were used as fillers or binder even for amorphous silica rather than as composite components. However, if it is present in high amounts resulting in an increase in porosity and an excess amount of amorphous silica. The remaining $Ca(OH)_2$ was found in T1 and T5 samples after soaking in water and salt solution. In the case of geopolymer mortar, $Ca(OH)_2$ can react with SiO_2 from silica fume or RHA to form calcium silicate hydrate gel (C-S-H gel) which decreases the porosity of the mortar as well as contribute to improvement in strength and durability. Additionally, the compressive strength of $FASiO_2$ was highest in this study because the average particle size of silica fume is smaller than RHA contributed to fill in the porosity of mortar. Figures 10 and 11 show the results of FESEM micrographs and EDS spectra of inside and outside samples for T1 and T5 soaked in the salt solution, respectively. After soaking in the salt solution, it found that there were not significantly different of T1 and T5 samples. It should be noted that Si, Al, and Ca contents significantly decreased, and Mg content remarkably increased on outside

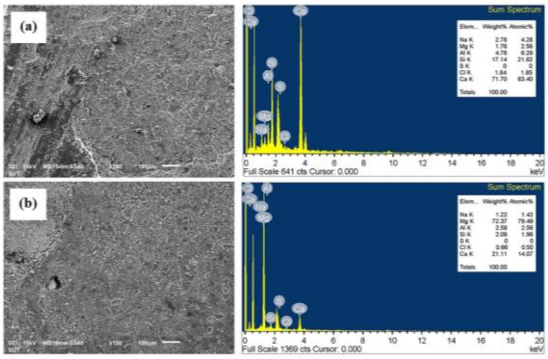

Figure 10. FESEM micrographs and EDS spectra of T1 sample soaked in the salt solution for 14 days (a) inside (100X) and (b) outside (100X)

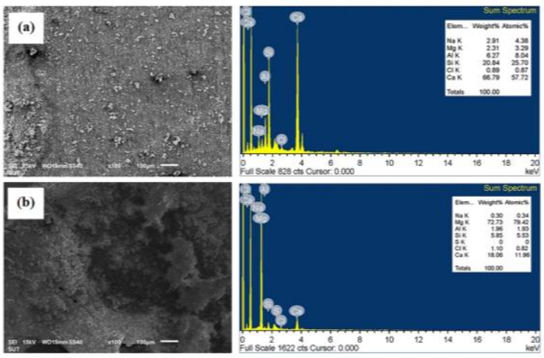

Figure 11. FESEM micrographs and EDS spectra of T5 sample soaked in the salt solution for 14 days (a) inside (100X) and (b) outside (100X)

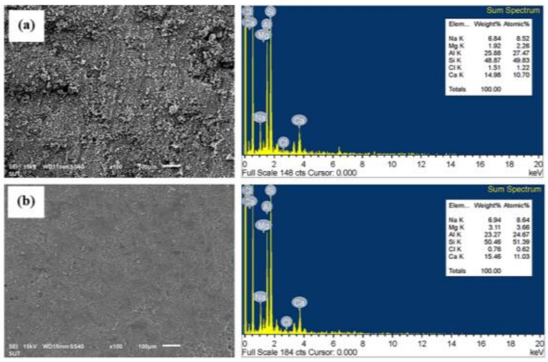

Figure 12. FESEM micrographs and EDS spectra of FA geopolymer soaked in the salt solution for 14 days (a) inside (100X) and (b) outside (100X)

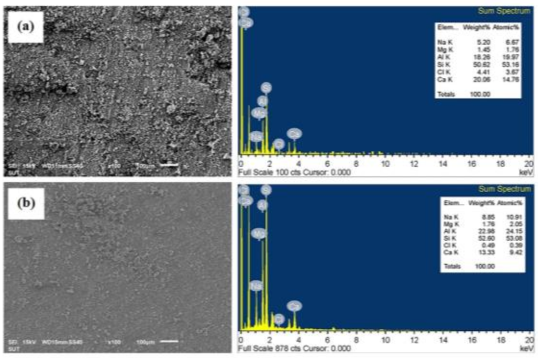

Figure 13. FESEM micrographs and EDS spectra of $FASiO_2$ geopolymer soaked in the salt solution for 14 days (a) inside (100X), (b) outside (100X)

samples soaked in the salt solution (Figures 10(b) and 11(b), respectively). Interestingly, FESEM-EDS results of inside and outside samples for FA and $FASiO_2$ geopolymers showed not notable change after soaking in the salt solution as shown in Figures 12 and 13, respectively.

The microstructure of all samples showed the fine structure with densify body. T5 showed that the magnesium (Mg) content was lower than that in T1, especially for outside of samples. It could indicate that T5 could protect Mg, Cl and S penetration into the cement as comparison to T1. Interestingly, FA and $FASiO_2$ geopolymer showed the lowest Mg, Cl and S content in both of inside and outside of the sample after soaking in the high concentrations of salt solution. $MgSO_4$ from seawater can react with calcium monosulfate aluminate with the presence of $Ca(OH)_2$ to produce ettringite causing the expansion stress in mortar and reducing the compressive strength for ordinary Portland cement. In the previous study conducted by Ekaputri *et al*. (2019), it was found that chloride was observed to form minerals bound with unreacted compounds such as calcium chloride and magnesium chloride. This proves that the binding capacity of geopolymer to bind to the ion chloride in concrete causes the chloride penetration to not produce free ions in geopolymer concrete. It should be noted that $FASiO_2$ should be adjusted the liquid and powder ratio for obtaining high densified body and its potential used for geopolymer with good salt resistance.

Another investigation showed that geopolymer concrete has a good development of compressive strength in aggressive environment for a long term. The chloride diffusion rate in geopolymer concrete is dependent on the porosity of the geopolymer matrix, which is governed by the reactivity of the precursor fly ash. The reactivity is dependent upon surface area, amorphous Al_2O_3 and SiO_2 content and CaO content. Higher surface area and amorphous Al_2O_3 and SiO_2 increase aluminosilicate gel formation and produce a stronger, less porous geopolymer matrix which reduces the rate of chloride ingress (Gunasekara *et al*., 2019) During the geopolymerisation process, silica and alumina in fly ash dissolve with NaOH to form sodium-alumina-silicate, which contributes to the strength of geopolymer concrete. The compressive strength on OPC was decreased because portlandite ($Ca(OH)_2$) leaks out from OPC concrete. Then, this compound bonds with NaCl to form calcium chloride ($CaCl_2$) which then reacts with aluminate in the cement. As a result, this reaction forms Friedle salt ($3CaO.Al_2O_3.CaCl_2.10H_2O$) which fills the pores. Chloride in salt water can cause cracks and accumulation of salt crystal as well (Halim *et al*., 2017). It also happened on the compressive strength of geopolymer concrete which was immersed in salt water (Singh, 2018). The measurement of chloride penetration was intended to determine the depth of concrete that has been damaged by chloride ions. This indicates that there is a correlation between porosity and chloride penetration. The greater the total porosity, the more chloride ion penetrate to concrete. Geopolymer concrete has higher compressive strength than OPC in salt water.

Conclusions

This study aimed to enhance the chloride and sulfate resistance of cement by investigating the use of geopolymer with waste materials such as fly ash, silica fume, and rice husk ash. Chemical and microstructural analyses were conducted to understand the mechanisms and chemical reactions of geopolymer when exposed to salt solution as compared to water immersion. The geopolymer mortar made from fly ash, as well as the combination of fly ash and silica fume, exhibited higher compressive strength than OPC type 1 and type 5. Furthermore, the geopolymer mortar with the combination of fly ash and silica fume showed improving resistance to salt. Overall, the geopolymer used in this study was lightweight, friendly environmental, and cost-effective, making it a viable option for alternative concrete applications.

Acknowledgement

This study acknowledge support provided by Fundamental Fund (FF) from National Research Council of Thailand (NRCT), (i) Suranaree University of Technology (SUT), (ii) Thailand Science Research and Innovation (TSRI), (iii) National Science, Research and Innovation Fund (NSRF) (project code 90464) and finally, the authors would like to thank NWN trading and SIE-CON for raw materials (fly ash) support.

References

Amin, M. and Abdelsalam, B.A. (2019). Efficiency of rice husk ash and fly ash as reactivity materials in sustainable concrete. Sustainable Environment Research, 29:30. https://doi.org/10.1186/s42834-019-0035-2

Bumanis, G., Bajare, D., Korjakins, A., and Vaičiukynienė, D. (2022). Sulfate and freeze-thaw resistance of porous geopolymer based on waste clay and aluminum salt slag. Minerals, 12(9):1140. https://doi.org/10.3390/min12091140

Chaitanya, M.S.K., Nagaraju, T.V., Gadhiraju, L.V.K.R., Madepalli, V.R., and Jampana, S.N.R. (2023). Strength and micro-structural performance of geopolymer concrete using highly burned rice husk ash. Materials Today: Proceedings, 86. https://doi.org/10.1016/j.matpr.2023.04.617

Chanakya Varma, V., Nagaraju, T.V., Raju, J.N.S.S.N., Alisha, S.S., and Chaitanya, M.S.K. (2023). Understanding the potential role of precursor content in the geopolymer concrete strength development. Materials Today: Proceedings, https://doi.org/10.1016/j.matpr.2023.05.227

Davidovits, J. (1994). Global warming impact on the cement and aggregates industries. World Resource Review, 6(2):263.

Ekaputri, J.J., Lie, H.A., Fujiyama, C., Shovitri, M., Alami, N.H., and Setiamarga, D.H.E. (2019). The effect of alkali concentration on chloride penetration in geopolymer concrete. In: 7th International Conference on Euro Asia Civil Engineering Forum, 30 September - 2 October, 2019; Stuttgart; Germany, 615:012114. https://doi.org/10.1088/1757-899X/615/1/012114

Gunasekara, C., Law, D., Bhuiyan, S., Setunge, S., and Ward, L. (2019). Chloride induced corrosion in different fly ash based geopolymer concretes. Construction and Building Materials, 200:502-513. https://doi.org/10.1016/j.conbuildmat.2018.12.168

Halim, L.N., Ekaputri, J.J., and Triwulan, T. (2017). The influence of salt water on chloride penetration in geopolymer concrete. MATEC Web of Conferences, 97:01002. https://doi.org/10.1051/matecconf/20179701002

Jaya, P.R., Nor, M.A.A.M., Ahmad, Z.A., and Amin, Z.M. (2013). Properties of mortar containing rice husk ash at different temperature and exposed to aggressive environment. Advanced Materials Research, 620:87-93. https://doi.org/10.4028/www.scientific.net/AMR.620.87

Ken, P.W., Ramli, M., and Ban C.C. (2015). An overview on the influence of various factors on the properties of geopolymer concrete derived from industrial by-products. Construction and Building Materials, 77:370-395. https://doi.org/10.1016/j.conbuildmat.2014.12.065

Krishnam Raju, G.L.V., Vamsi Nagaraju, T., Jagadeep, K., Venkata Rao, M., and Chanakya Varma, V. (2023). Waste-to-energy agricultural wastes in development of sustainable geopolymer concrete. Materials Today: Proceedings, https://doi.org/10.1016/j.matpr.2023.05.481

Meesala, C.R., Verma, N.K., and Kumar, S. (2020). Critical review on fly-ash based geopolymer concrete. Structural Concrete Journal, 21(3):853-1207. https://doi.org/10.1002/suco.201900326

Nagaraju, T.V., Bahrami, A., Azab, M., and Naskar, S. (2023a). Development of sustainable high performance geopolymer concrete and mortar using agricultural biomass-A strength performance and sustainability analysis. Frontiers in Materials, 10:1128095. https://doi.org/10.3389/fmats.2023.1128095

Nagaraju, T.V., Malegole, S.B., Chaudhary, B., and Ravindran, G. (2022). Assessment of environmental impact of aquaculture ponds in the western delta region of Andhra Pradesh. Sustainability, 14(20):13035. https://doi.org/10.3390/su142013035

Nagaraju, T.V., Mantena, S., Azab, M., Alisha, S.S., El Hachem, C., Adamu, M., and Murthy, P.S.R. (2023b). Prediction of high strength ternary blended concrete containing different silica proportions using machine learning approaches. Results in Engineering, 17:100973. https://doi.org/10.1016/j.rineng.2023.100973

Olivia, M. and Nikraz, H. (2012). Properties of fly ash geopolymer concrete designed by Taguchi method. Materials & Design (1980-2015), 36:191-198. https://doi.org/10.1016/j.matdes.2011.10.036

Sambucci, M., Sibai, A., and Valente, M. (2021). Recent advances in geopolymer technology. A potential eco-friendly solution in the construction materials industry: A review. Journal of Composites Science, 5(4):109. https://doi.org/10.3390/jcs5040109

Sathawane, S.H., Vairagade, V.S., and Kene, K.S. (2013). Combine effect of rice husk ash and fly ash on concrete by 30% cement replacement. Procedia Engineering, 51:35-44. https://doi.org/10.1016/j.proeng.2013.01.009

Shaikh, F.U.A. (2014). Effects of alkali solutions on corrosion durability of geopolymer concrete. Adv. Concr. Constr., 2(2):109-123. https://doi.org/10.12989/acc.2014.2.2.109

Singh, N.B. (2018). Fly ash-based geopolymer binder: A future construction material. Minerals, 8(7):299. https://doi.org/10.3390/min8070299

Singh, N.B. and Middendorf, B. (2020). Geopolymers as an alternative to Portland cement: An overview. Construction and Building Materials, 237:117455. https://doi.org/10.1016/j.conbuildmat.2019.117455

Singh, N.S., Thokchom, S., and Debbarma, R. (2021). Properties of fly ash and rice husk ash blended geopolymer with sodium aluminate as activator solution. Engineering and Applied Science Research, 48(1):92-101.

Umbach, C., Wetzel, A., and Middendorf, B. (2021). Durability properties of ultra-high performance lightweight concrete (UHPLC) with expanded glass. Materials, 14(19):5817. https://doi.org/10.3390/ma14195817

Živica, V., Palou, M.T., and Križma, M. (2015). Geopolymer cements and their properties: a review. Building Research Journal, 61(2):85-100. https://doi.org/10.2478/brj-2014-0007